Interstellar Ice Surface Site Modification Induced by Dicyanoacetylene Adsorption

Zohra Guennoun, Isabelle Couturier-Tamburelli,* Nathalie Piétri, and Jean-Pierre Aycard

UMR CNRS 6633, Physique des Interactions Ioniques et Moléculaires, Equipe de Spectrométries et Dynamique Moléculaires, Université de Provence, Case 252, Centre de St-Jérôme, 13397 Marseille Cedex 20, France

Received: November 3, 2004; In Final Form: December 14, 2004

Dicyanoacetylene adsorbed on amorphous ice water at 10 K presents an interaction with the dangling H site and induces a s_4 adsorption site formation due to the restructuring of the ice bulk. Warming up the sample provokes the dicyanoacetylene desorption from the H_2O ice film, which could be due to the beginning of the ice crystallization process. The desorption activation energy measured by temperature-programmed desorption ($E_d = 42 \pm 5$ kJ·mol^{-1}) is in good agreement with that calculated ($E_d = 46$ kJ·mol^{-1}) and gives evidence of a hydrogen-bonded adsorbed state on amorphous ice films.

Introduction

With the arrival of a Cassini-Huygens orbiter and probe in January 2005,[1] the interest of the Titan atmosphere simulations grows because this mission will provide numerous additional data on both gaseous and solid phases. Indeed, this largest satellite of Saturn is the only one in the solar system presenting a dense atmosphere.[1−2] The main compounds nitrogen and methane[1] react upon solar UV radiations producing mainly molecules including nitriles such as dicyanoacetylene. Moreover, the H_2O molecule, which could be issued from cometary's contribution, has been recently detected[3] in this satellite. It is now well-known that, in the interstellar medium, heterogeneous reactions are developed on ice surfaces or in the icy mantle of the grains,[4] which are assumed to play an important role in interstellar chemistry.[5]

Therefore, following our previous works[6] on polycyanoethyne chemistry, we report here original experiment results on the interactions between dicyanoacetylene, C_4N_2, and amorphous water ice surface.

In the solid state, each H_2O molecule can form four hydrogen bonds (two as a proton donor and two as a proton acceptor) with four other H_2O molecules.[7] Three kinds of surface molecules have been characterized: two for three-coordinated molecules and one for four-coordinated molecules. Three-coordinated H_2O molecules with an OH group noninvolved in a hydrogen bond are referred to molecules with a dangling H (d_H), using Devlin's notation. Three-coordinated H_2O molecules, with an oxygen electronic lone pair noninvolved in a hydrogen bond, are referred to molecules with a dangling O (d_O). At last, four-coordinated H_2O molecules leaving neither H nor lone pair free are referred to s_4 sites.

In a previous paper,[6a] we present the results on the structure and energy of the 1:1 complexes formed between dicyanoacetylene and water in argon matrix. Two types of 1:1 complexes are observed: the first one named NH is characterized by a hydrogen bond between H_2O and one of the nitrogen atoms of dicyanoacetylene; the second, called CO, displays a van der Waals interaction between the Cβ of dicyanoacetylene and the oxygen atom of water.

* Author to whom correspondence may be addressed. E-mail: isabelle.couturier@up.univ-mrs.fr. Phone: (+33) 4-91-28-28-16. Fax: (+33) 4-91-63-65-10.

The purpose of this work is to assess the chemical stability of C_4N_2 adsorbed on amorphous water ice surface, model of interstellar ices.

Experimental Section

Pure dicyanoacetylene was synthesized using the method described by Moureu and Bongrand.[8] The dicyanoacetylene is distilled before each deposition. Moreover, the first fraction of C_4N_2 is evacuated.

H_2O was doubly distilled before use and degassed by successive freeze−thaw cycles under vacuum before each use.

Low-density amorphous ice films are obtained from a water/argon (1/50) gaseous mixture deposited on a highly polished Cu-plated gold cube held at 80 K. The deposition is made under a constant pumping of 10^{-7} mbar in order to outgas Ar to obtain a porous solid.[9] Then the film is cooled to 10 K to deposit pure C_4N_2 and to study the adsorption process. Adsorption and desorption of dicyanoacetylene on the amorphous ice film were monitored by IR spectroscopy using a Nicolet series II Magna system 750 in the 4000−600-cm^{-1} wavenumber range at a resolution of 1 cm^{-1}.

IR spectra of amorphous ice have been extensively described in the literature.[10] The amorphous nature is characterized first by the shape of the broad band centered at 3250 cm^{-1} and second by the weak band at 3695 cm^{-1} (d_H). Two other vibrational surface modes are present at 3549 and 3503 cm^{-1}, which are attributed to the d_O and s_4 sites, respectively, by Manca et al.[11] During a temperature increase, an irreversible modification of the amorphous ice toward crystalline form was observed near 145 K. Ice remains its crystalline feature, until the sample sublimates at 180 K. This form is characterized by two shoulders[12] at 3340 and 3150 cm^{-1} on the large profile of the ν_{OH} mode at 3260 cm^{-1}.

Several temperature-programmed desorption (TPD) experiments, adapted to Fourier transform IR spectroscopy as previously described,[13] were conducted using different heating rates (β). For each of them, we can evaluate the fractional surface coverage from the normalized integrated absorbance of the dicyanoacetylene vs *T*.

Results and Discussion

Adsorption and Desorption of C_4N_2 on Amorphous Ice. As described in the Experimental Section, amorphous ice

10.1021/jp044978k CCC: $30.25
Published on Web 01/29/2005

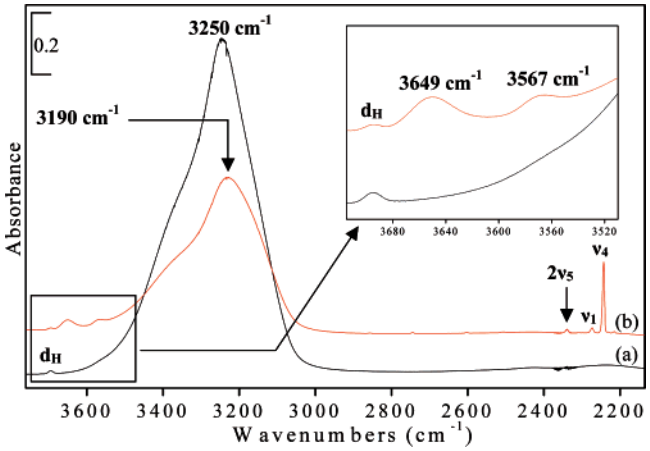

Figure 1. IR spectra resulting from a C_4N_2 exposure on an amorphous ice film maintained at 10 K: (a) bare amorphous ice; (b) after C_4N_2 adsorption on ice.

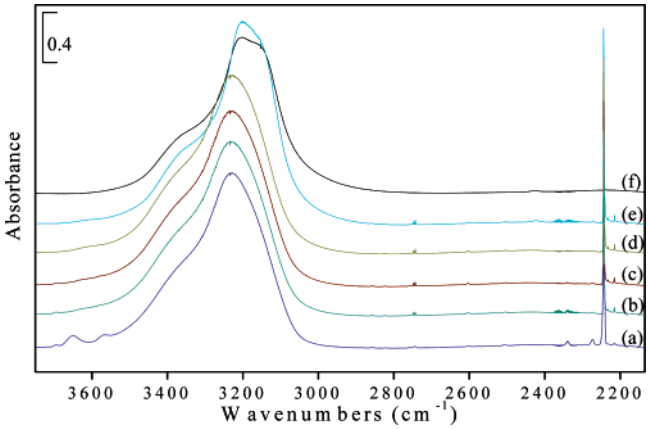

Figure 2. Selected IR spectra during the TPD ($\beta = 0.8$ K min^{-1}) of C_4N_2 from amorphous ice surface in the OH stretching region of ice and in the ν_4 mode region of C_4N_2: (a) 10 K; (b) 80 K; (c) 100 K; (d) 130 K; (e) 150 K; (f) 170 K.

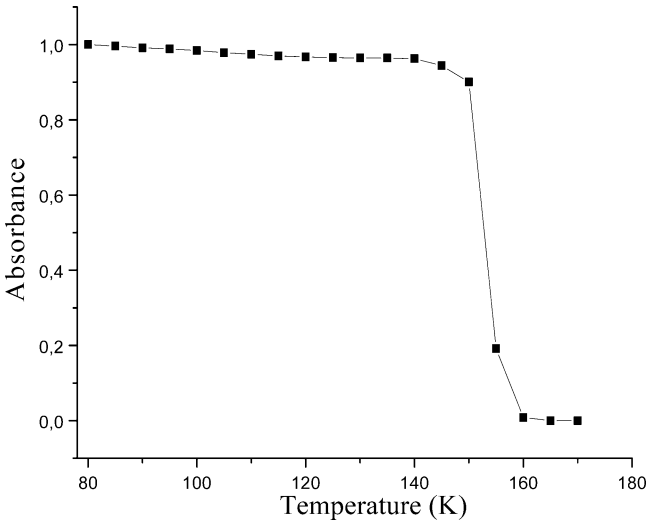

Figure 3. Integrated normalized absorbance of the ν_4 mode of C_4N_2 with temperature ($\beta = 0.8$ K min^{-1}) following the results presented in Figure 3.

displays a weak feature at 3695 cm^{-1}, which is due to the dangling H mode (d_H). This latter is generally used to follow adsorption of molecules on ice surfaces. The C_4N_2 adsorption on a bare amorphous ice film at 10 K results in a decrease but not the total disappearance of the d_H band. During this desorption, two bands located at 3649 and 3567 cm^{-1} grow. The first one results in a downshift of 46 cm^{-1} of the free OH stretching mode (Figure 1). As with C_3O_2, acetone ... this large shift[12,14] indicates a strong interaction between C_4N_2 and the ice film. Another band appears at 3567 cm^{-1}, located in the d_O (3549 cm^{-1}) and s_4 (3503 cm^{-1}) site areas for the bare ice.[11,15] These two bands situated at 3649 and 3567 cm^{-1} appear as soon as the first fraction of C_4N_2 is deposited. They can probably be attributed to weak and strong d_H interactions with the C_4N_2 or a d_H interaction and another type of interaction between C_4N_2 and ice.

In the same way during the adsorption, we observe a major modification in the ice surface. Indeed, the intensities of the bulk OH stretching and bending modes at 3250 and 1660 cm^{-1} are shifted to lower frequencies by 60 and 40 cm^{-1}, respectively (Figure 1). We therefore assume that these frequency shifts could be due to a major modification of ice, induced by the C_4N_2 adsorption.

Recent works[11,16] have shown that CO, CH_4, and rare gas atoms (Ar, Kr) adsorbed on d_O and s_4 lead to a decrease in the IR responses of these sites. Nevertheless, in our experiment, we observe that a band is formed at 3567 cm^{-1} (Figure 1). Thus, we hypothesize that C_4N_2 adsorption leads to the d_O or s_4 site formation due to the restructuring of the ice bulk.

Furthermore, it should be noted that the d_H IR does not totally disappear when the C_4N_2 is adsorbed. In fact, the C_4N_2 molecule is probably too long to penetrate into every pore.

Nevertheless, C_4N_2 adsorption on amorphous ice surface induces only a broadening but no change in the position of the IR C_4N_2 absorption bands. The line shapes and the positions of the ν_4 and ν_5 modes of C_4N_2, situated at 2243 and 1159 cm^{-1}, respectively, are the same as those observed in the spectrum of pure solid dicyanoacetylene.[17]

Figure 2 shows selected spectra recorded during the sample annealing from 15 K to C_4N_2 sublimation temperature with a β heating rate of 0.4 K min^{-1}. Above 85 K, the d_H signal begins to decrease in intensity and then disappears at 130 K. The latter phenomenon is due to the collapse of amorphous ice pores during their evolution in crystalline ice. The desorption process can be followed in Figure 3, showing the ν_4 integrated band intensity variations. Between 80 and 145 K, the peak intensity is unchanged, which is indicative of a stable adsorption state. At 150 K, we observe an abrupt decrease that results from the sublimation of adsorbed C_4N_2. It is noteworthy first that this sublimation occurs at the beginning of the ice crystallization process near the phase-transition temperature and second that it occurs in a temperature range below those obtained for solid C_4N_2 ($\cong$170 K).

The C_4N_2 desorption follows a first-order kinetic model. To estimate the activation desorption energy of C_4N_2 from the amorphous ice, we performed a TPD study[13] using five β values taken between 0.4 and 1.2 K·min^{-1}. T_p (temperature for which the desorption is maximal) is evaluated for each heating rate. From the linear plotting of ln β/RT_p^2 vs $1/T_p$ (Figure 4), we determined $E_d = 42 \pm 5$ kJ·mol^{-1} and $A_d = 10^{13}$ s^{-1} values. This activation desorption energy (E_d) value is lower than that evaluated by TPD experiments for solid C_4N_2 desorption from the cryostat surface of 51 ± 5 kJ·mol^{-1}. At last, the activation desorption energy ($E_d = 42 \pm 5$ kJ·mol^{-1}) measured from the C_4N_2 desorption of the ice surface is consistent with the existence of two hydrogen bonds between the ice surface and the C_4N_2 moiety.

Theoretical Study of Adsorption of C_4N_2 on Ice. Our experimental results are indicative of an adsorption of the

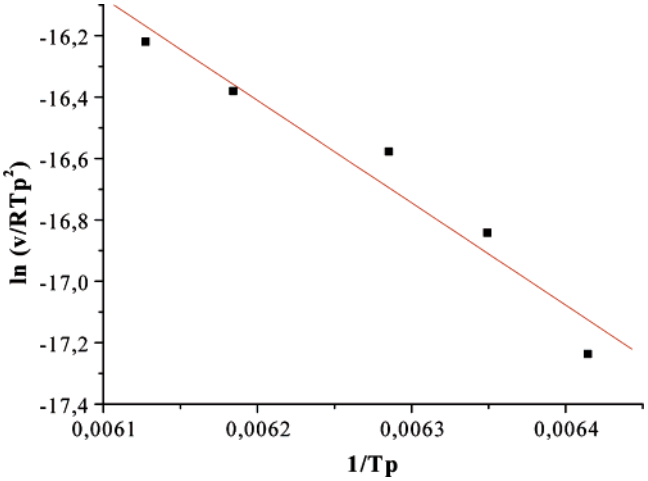

Figure 4. Desorption kinetics of C_4N_2 from amorphous ice surface obtained for five TPD experiments. The line is derived from a linear regression analysis of the data points.

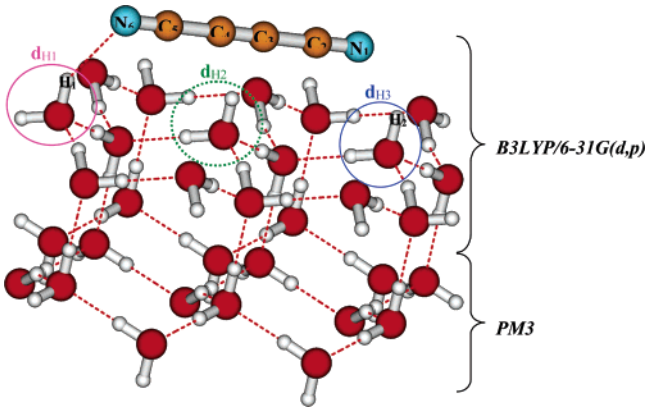

Figure 5. Starting configuration for theoretical calculation of C_4N_2 adsorbed on amorphous ice surface.

dicyanoacetylene molecule on dangling H sites of amorphous ice surface. To reinforce our adsorption results, to confirm the d_O or s_4 formation, and to modelize the structure of C_4N_2 adsorbed, we perform theoretical calculations.

The whole system (C_4N_2 + ice) was considered as a two-domain system. Indeed, the calculations were performed using the Gaussian 03 package of programs,[18] the ONIOM method in the B3LYP/6-31G** formalism[19] for the high-level system (constituted by the adsorbed molecule and the upper ice layer), and semiempirical Hartree−Fock method for the low level (constituted by the lower ice layer, Figure 5).

However, it is well-known that weaker interactions are partly estimated from DFT functional, which contain some unphysical self-interaction. At the molecular level, Möller−Plesset generally gives better results, but it is not yet applicable to the 3D crystalline model.[20]

The entire system (C_4N_2 + ice) was optimized without any restriction, taking into account the relaxation of the structure surface. To lower the calculations cost required by this system, we only use two layers for the ice surface.

The ice that we considered is the protonic ordered periodic ice structure P as determined and optimized by Pisani et al.[21] This theoretical model is well adapted for studying adsorption on amorphous ice surfaces and has been used with success in earlier papers.[22] In the present work, the ice surface is represented by a slab of two molecular bilayers, periodic in the two dimensions, parallel to the [0 0 0 1] face and labeled P(2) ice (Figure 5). Moreover, due to the large size of the C_4N_2 molecule (~6.3 Å, theoretically) compared to the unit cell parameters, we proceeded with a double supercell.

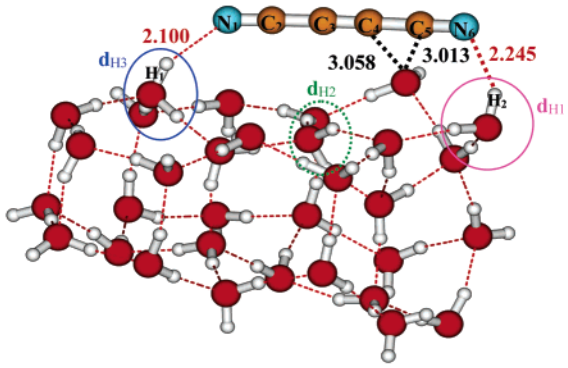

Figure 6. Optimized structure of C_4N_2 interacting with ice surface obtained by theoretical calculations. The lengths are given in angstroms.

At last, the adsorption energy is calculated using the following equation:

$\Delta E = E(C_4N_2 + \text{ice}) - E^{BSSE}(C_4N_2) - E^{BSSE}(\text{ice})$, where $E^{BSSE}(C_4N_2)$ and $E^{BSSE}(\text{ice})$ are the energies of the dicyanoacetylene and the ice surface corrected of the basis set superposition error (BSSE).[23]

We have explored two positions of C_4N_2 interacting with the amorphous ice to determine the nature of the adsorption sites. The first structure displays the C_4N_2 moiety upright above the dangling H site. The second one shows the C_4N_2 flattened on the ice surface in interaction with three dangling H sites (Figure 5). Indeed, by analogy with the structure of one of the C_4N_2:H_2O complexes formed in the argon matrix,[6a] the C_4N_2 molecule is placed with the terminal nitrogen interacting with two free OH bonds of the ice surface (denoted d_{H1} and d_{H3} in Figure 5) while the acetylenic system of C_4N_2 is also in interaction with one of these sites (d_{H2}, Figure 5). H/π interaction between dicyanoacetylene and water does not lead to a stable complex structure, and this kind of complex is not observed in matrix.[6a]

The two starting positions considered converge toward the same minimum. In this structure, the dicyanoacetylene is flattened on ice surface and is stabilized by two hydrogen bonds (Figure 6), which are formed between the nitrogen atoms of C_4N_2 (N_1 and N_6) and two dangling Hs (d_{H1} and d_{H3}). The former is calculated to be 2.100 Å in length, and the latter, for which the nitrogen of the adsorbed molecule interacts more weakly with the ice dangling H, is about 2.245 Å.

In addition, the optimized geometry exhibits two van der Waals interactions between the carbon atoms (C_4 and C_5) of the C_4N_2 moiety and the oxygen atom of a H_2O surface molecule (Figure 6). The atoms involved in these interactions are distant of 3.058 and 3.013 Å, respectively.

It is worthwhile to note that the interactions formed between C_4N_2 and the ice surface are in close vicinity to those observed in an argon matrix between the dicyanoacetylene and the water subunits. Indeed, as already described in the introduction, in the argon matrix, we have characterized two kinds of interactions between C_4N_2 and H_2O leading to NH and CO complexes.[6a]

Furthermore, the comparison between the starting P ice and our optimized structure shows that the adsorption of C_4N_2 on ice surfaces leads to the disappearance of the d_{H2} dangling H site. Indeed, the interaction between the acetylenic system of C_4N_2 and the free OH bond has disappeared. The d_{H2} flipping provokes the formation of a new four-coordinated water molecule (s_4 site).[7] This result is in good agreement with the growing of the band at 3567 cm^{-1} in the s_4 sites region in our experiment. Thus, this band is due to the creation of s_4

TABLE 1: Desorption Peak Maximum Temperatures (T_p) for Various Heating Rates (β)

heating rate β (K·min^{-1})	T_p (K)
0.4	155.9
0.6	157.5
0.8	159.1
1.0	161.7
1.2	163.2

TABLE 2: Optimized Structural Parameters for the C_4N_2 Adsorbed on an Amorphous Ice Surface Obtained by Theoretical Calculations[a]

parameters	free C_4N_2	d_H sites of ice	C_4N_2 adsorbed on ice surface
rN_1C_2	1.167		1.166
rC_2C_3	1.366		1.366
rC_3C_4	1.217		1.216
rC_4C_5	1.366		1.365
rC_5N_6	1.167		1.166
$\angle N_1C_2C_3$	180.0		178.6
$\angle C_2C_3C_4$	180.0		178.1
$\angle C_3C_4C_5$	180.0		176.7
$\angle C_4C_5N_6$	180.0		176.7
rOH_1		0.967	0.971
rOH_2		0.967	0.967
ΔE(BSSE)			−46.2

[a] Bond lengths are given in angstroms and angles in degrees. The energy ΔE is given in kJ·mol^{-1}.

adsorption site when dicyanoacetylene is adsorbed on amorphous ice water.

We report in the Table 2 the optimized geometrical parameters of the dicyanoacetylene and the dangling H sites (d_{H1} and d_{H3}) involved in the hydrogen bonding. The analysis of these data points out that the bond lengths of the C_4N_2 adsorbed on ice water are nearly unchanged with respect to the monomer structure. The valence bond angles are slightly modified from 2 to 4°. Since the structural parameters are in close vicinity with those of the free molecule, slight shifts of the absorption bands are observed.

By consideration of the clusters that support this calculation, the d_{H2} site is assumed to be unaffected, and only the OH bond length of the d_{H1} site is perturbed by the adsorption (Table 2). Indeed, this latter is longer than that of the bare ice by 0.004 Å. This coordinate leads to a downshift, which is about 59 cm^{-1} with respect to the free d_H of the bare ice. It is important to note the good agreement between the experimental shift $\Delta\nu$, 46 cm^{-1} [ν nonperturbed d_H (3695 cm^{-1}) − ν perturbed d_H by C_4N_2 adsorption (3649 cm^{-1})], and the theoretical one, 59 cm^{-1} [ν nonperturbed d_H (3834 cm^{-1}) − ν perturbed d_H by C_4N_2 adsorption (3775 cm^{-1})].

It is worth noting note that the adsorption of C_4N_2 on the amorphous surface water leads to dramatic modifications of the ice structure after optimization (Figure 6). This result is consistent with the absorption bands shifts of the bulk OH stretching and bending modes, observed in our experiment (60 and 40 cm^{-1}, respectively).

At last, the interaction energy was calculated (using BSSE correction[23]) to be −46 kJ·mol^{-1}, which is in good agreement with the experimental adsorption energy measured to be −42 kJ·mol^{-1} by TPD experiments.

Conclusion

In conclusion, the present study shows that C_4N_2 is stable on ice until 150 K, which is consistent with interstellar medium conditions. The evolution of the integrated absorbance of the IR bands shows that C_4N_2 desorbs from the amorphous ice surface in the 150−165 K range of temperature. C_4N_2 is adsorbed on amorphous ice surface by its nucleophilic nitrogen atoms of the cyano groups. The C_4N_2 is flattened on the ice surface and stabilized by two hydrogen bonds of 2.100 and 2.245 Å in length. The calculated adsorption energy (46 kJ·mol^{-1}) is in the same order of magnitude as the experimental one (42 ± 5 kJ·mol^{-1}). The adsorption of dicyanoacetylene on amorphous ice surface induces a major restructuring of the ice bulk and the growing of two bands at 3649 and 3567 cm^{-1}. The former band is due to the interaction between the d_H and the nitrogen atoms of C_4N_2. The same phenomenon has already been observed when C_3O_2 is adsorbed on ice surface.[22b] The calculation shows that the C_3O_2 subunit is flattened on the ice surface, the two terminal oxygen interacting with two free OH bonds of the ice surface. Nevertheless, only one d_H shift response is observed. Thus, the second band, observed at 3567 cm^{-1} in our experiment, is assigned to s_4 site formation by comparison with the calculation data. This s_4 site formation was never previously observed to our knowledge.

Acknowledgment. The theoretical part of this work was conducted with the technical means of "Centre régional de Compétence en Modélisation Moleculaire de Marseille".

References and Notes

(1) Bernard, J. M.; Coll, P.; Coustenis, A.; Raulin, F. *Planet. Space Sci.* **2003**, *51*, 1003.

(2) Israel, G.; Cabane, M.; Coll, P.; Coscia, D.; Raulin, F.; Hiemann, H. *Adv. Space Res*. **1999**, *23*, 319.

(3) Coustenis, A.; Salama, A.; Lellouch, E.; Encrenaz, Th.; Bjoraker, G. L.; Samuelson, R. E.; De Graauw, Th.; Feuchgruber, H.; Kessler, M. F. *Astron. Astrophys*. **1998**, *336*, L85.

(4) D'Hendecourt, L.; Jourdain de Muizon M.; Dartois, E.; Breitfellner, M.; Freud, P.; Benit, J.; Boulanger, F.; Puget, J. L.; Habing, H. J. *Astron. Astrophys*. **1996**, *315*, L365.

(5) Graham, J. D.; Roberts, J. T. *J. Phys. Chem. B* **2000**, *104*, 978.

(6) (a) Guennoun, Z.; Piétri, N.; Couturier-Tamburelli, I.; Aycard, J. P. *Chem. Phys*. **2004**, *300*, 23. (b) Borget, F.; Chiavassa, T.; Allouche, A.; Marinelli, F.; Aycard, J. P. *J. Am. Chem. Soc*. **2001**, *123*, 10668. (c) Casassa, S.; Ugliengo, P.; Pisani, C. *J. Chem. Phys*. **1997**, *106*, 8030.

(7) (a) Borget, F.; Chiavassa, T.; Aycard, J. P. *Chem. Phys. Lett*. **2001**, *348*, 425. (b) Devlin, J. P.; Buch, V. *J. Phys. Chem*. **1995**, *99*, 16534. (c) Devlin, J. P.; Buch, V. *J. Phys. Chem. B* **1997**, *101*, 6095.

(8) Moureu, C.; Bongrand, J. C. *Ann. Chim.* **1920**, *14*, 47.

(9) (a) Givan, A.; Loewenshuss, A.; Nielsen, C. *J. Phys. Chem. B* **1997**, *101*, 8696. (b) Givan, A.; Loewenshuss, A.; Nielsen, C. *Chem. Phys. Lett.* **1997**, *275*, 98.

(10) Rowland, D.; Devlin, J. P. *J. Chem. Phys*. **1991**, *94*, 812.

(11) Manca, C.; Martin, C.; Roubin, P. *Chem. Phys.* **2004**, *300*, 53.

(12) Graham, J. D.; Roberts, J. T. *Geophys. Res. Lett*. **1995**, *22*, 251.

(13) Couturier-Tamburelli, I.; Chiavassa, T.; Pourcin, J. *J. Phys. Chem. B* **1999**, *103*, 3677.

(14) Schaff, J. E.; Roberts, J. T. *J. Phys. Chem.* **1996**, *100*, 14151.

(15) (a) Devlin, J. P.; Buch, V. *J. Phys. Chem*. **1995**, *99*, 16534. (b) Devlin, J. P.; Buch, V. *J. Phys. Chem*. **1997**, *101*, 6095.

(16) (a) Manca, C. Thèse de l'Université de Provence, 2002. (b) Manca, C.; Martin, C.; Allouche, A.; Roubin, P. *J. Phys. Chem. B* **2001**, *105*, 12861.

(17) (a) Khanna, R. K.; Perera-Jarmer, M. A.; Ospina, M. J. *Spectrochim. Acta A* **1987**, *43*, 421. (b) Miller, F. A.; Hannan, R. B., Jr. *J. Chem. Phys*. **1953**, *21*, 110. (c) Miller, F. A.; Hannan, R. B., Jr.; Cousins, L. R. *J. Chem. Phys*. **1955**, *23*, 2127.

(18) Frisch, M. J.; Trucks, G. W.; Schlegel, H. B.; Scuseria, G.; E.; Robb, M. A.; Cheeseman, J. R.;. Zakrzewski, V. G., Jr; Montgomery, J. A.; Stratmann, R. E.; Burant, J. C.; Dapprich, S.; Millam, J. M., Daniels, A. D.; Kudin, K. N.; Strain, M. C.; Farkas, O.; Tomasi, J.; Barone, V.; Cossi, M.; Cammi, R.; Mennucci, B.; Pomelli, C.; Adamo, C.; Clifford, S.; Ochterski, J.; Petersson, G. A.; Ayala, P. Y.; Cui, Q.; Morokuma, K.; Malick, K. D.; Rabuck, A. D.; Raghavachari, K.; Foresman, J. B.; Cioslowski, J.; Ortiz, J. V.; Baboul, A. G.; Stefanov, B. B.; Liu, G.; Liashenko, A.; Piskorz, P.; Komaromi, I.; Gomperts, R.; Martin, R. L.; Fox, D. J.; Keith, T.; Al-Laham, M. A.; Peng, C. Y.; Nanayakkara, A.; Gonzalez, C.; Challacombe, M.; Gill, P. M. W.; Johnson, B.; Chen, W.; Wong, M. W.; Andres, J. L.; Gonzalez, C.; Head-Gordon, M.; Replogle, E. S.; Pople, J. A. *Gaussian 03*; Gaussian, Inc.: Pittsburgh, PA, 2003.

(19) (a) Becke, A. D. *J. Chem. Phys.* **1993**, *98*, 5648. (b) Lee, C. W.; Yang, W. Parr, R. G. *Phys. Rev. B* **1988**, *37*, 785. (c) Möller C.; Plesset M. S. *Phys. Rev.* **1934**, *46*, 618.

(20) (a) Bussolin, G.; Casassa, S.; Pisani, C.; Ugliengo, P. *J. Chem. Phys.* **1998**, *108*, 9516. (b) Marinelli, F.; Allouche, A. *Chem. Phys.* **2001**, 137, 272.

(21) Pisani, C.; Casassa, S.; Ugliengo, P. *Chem. Phys. Lett.* **1996**, *1253*, 201.

(22) (a) Allouche, A. *J. Phys. Chem.* **1996**, *100*, 17915. (b) Allouche, A.; Couturier-Tamburelli, Chiavassa, T. *J. Phys. Chem. B*, **2000**, *104*, 1497.

(23) Boys, S.; Bernardi, F. *Mol. Phys.* **1970**, *19*, 553